Is distance from equilibrium a good indicator for a reaction's flux control?

van Niekerk, D.D.; Rust, E.; Bruggeman, F.; Westerhoff, H.V.; Snoep, J.L.

DOI
10.1016/j.biosystems.2023.104988

Publication date
2023

Document Version
Final published version

Published in
Biosystems

License
CC BY

BioSystems 232 (2023) 104988

Contents lists available at ScienceDirect

BioSystems

journal homepage: www.elsevier.com/locate/biosystems

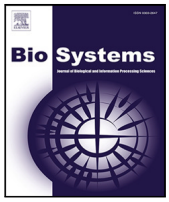

Is distance from equilibrium a good indicator for a reaction's flux control?

David D. van Niekerk [a], Erik Rust [a], Frank Bruggeman [b], Hans V. Westerhoff [b,c,d,e], Jacky L. Snoep [a,b,*]

[a] Department of Biochemistry, Stellenbosch University, South Africa
[b] Molecular Cell Biology, Vrije Universiteit Amsterdam, Amsterdam, The Netherlands
[c] Swammerdam Institute for Life Sciences, University of Amsterdam, Sciencepark 904, 1098 XH Amsterdam, The Netherlands
[d] School of Biological Sciences, Faculty of Biology, Medicine and Health, The University of Manchester, Manchester M13 9PT, UK
[e] Stellenbosch Institute of Advanced Studies (STIAS), Wallenberg Research Centre at Stellenbosch University, Stellenbosch 7600, South Africa

ARTICLE INFO

Keywords:
Metabolic control analysis
Non equilibrium thermodynamics
Rate-limiting step
Elasticity coefficients
Model databases

ABSTRACT

By analysing a large set of models obtained from the JWS Online and Biomodels databases, we tested to what extent the disequilibrium ratio can be used as an estimator for the flux control of a reaction, a discussion point that was already raised by Kacser and Burns, and Heinrich and Rapoport in their seminal MCA manuscripts. Whereas no functional relation was observed, the disequilibrium ratio can be used as an estimator for the maximal flux control of a reaction step. We extended the original analysis of the relationship by incorporating the overall pathway disequilibrium ratio in the expression, which made it possible to make explicit expressions for flux control coefficients.

1. Introduction

Metabolic Control Analysis (MCA; Kacser and Burns, 1973; Heinrich and Rapoport, 1974) is an excellent framework for systems biology studies. With its four central theorems it shows how systemic properties, such as flux and concentration control, can be expressed in terms of local characteristics of the enzymes, particularly their elasticity coefficients (e.g. Fell, 1997). As such, MCA allows one to understand a system's behaviour as a function of its catalytic components, and their interactions, the main goal of systems biology (Alberghina and Westerhoff, 2005).

Before the development of MCA, disequilibrium was often used to identify reactions that potentially control metabolic fluxes, as opposed to equilibrium reactions that cannot have flux control (e.g. Newsholme and Gevers, 1967). Rolleston has proposed a disequilibrium ratio of 0.2 to distinguish between equilibrium and non-equilibrium enzymes (Rolleston, 1972). Later, Rohwer and Hofmeyr (2010) proposed a much stronger separation, i.e. disequilibrium ratio smaller than 0.1 for far from equilibrium (kinetically controlled), and larger than 0.9 for reactions close to equilibrium (thermodynamically controlled reaction rates).

Whereas the classification between equilibrium and non-equilibrium enzymes can be helpful to identify potentially controlling enzymes, it does not give a quantitative measure for the extent of control. Flux control coefficients, are well-defined measures of the extent to which reactions in a pathway control the steady state flux through it and may be seen as the extent to which a step is flux or perhaps even rate limiting, and it is interesting to test how strong flux control coefficients correlate to the extent that a reaction is away from equilibrium. Such a correlation was already suggested in the founding papers of MCA, Kacser and Burns (1973), Heinrich and Rapoport (1974), and in later studies further comparisons between the two entities have been made (e.g. Westerhoff and van Dam, 1987; Noor et al., 2014; Dai and Locasale, 2018).

It is important to test the strength of the correlation, as the precision of the flux control coefficient comes at a cost. It is a tedious task to experimentally determine control coefficients (Groen et al., 1982; Jensen et al., 1993), and although it is straightforward with modern software tools to calculate control coefficients from detailed mathematical models, the construction of such models is reliant on detailed kinetic information, which, in particular for large reaction networks, is hard to come by. In contrast, it is easier to estimate the disequilibrium ratio, as it can be calculated from metabolite concentrations and equilibrium constants.

In the last two decades many detailed kinetic models have been published and made available in model databases (e.g. JWS Online Olivier and Snoep, 2004, Biomodels le Novere et al., 2006, and the Physiome model repository Lloyd et al., 2008). Although these databases and many other resources for construction and analysis of kinetic models, such as the FAIRDOMHub (Wolstencroft et al., 2017), Brenda (Chang

* Corresponding author.
E-mail address: jls@sun.ac.za (J.L. Snoep).

https://doi.org/10.1016/j.biosystems.2023.104988
Received 2 June 2023; Received in revised form 26 July 2023; Accepted 27 July 2023
Available online 2 August 2023

et al., 2020), SABIO-RK (Wittig et al., 2018) have good APIs, that are ideal for automated retrieval and comparative analyses of models, not many such comparisons have been made. Large scale analysis of models in the Biomodels database have been made in a few studies (e.g. Alm et al., 2015; Lambusch et al., 2018). In these studies the Biomodels API was used to retrieve the model from the database, and they were analysed in terms of annotation and structure. Not many large scale simulation analyses have been done to compare simulation characteristics between different models (see du Preez et al., 2008 for a comparative analysis of a relatively small subset of JWS Online models), although a large scale simulation analysis was done to compare simulation results obtained with the same model using different simulators (Bergmann and Sauro, 2008).

In this contribution we follow three approaches to examine the correlation between flux control and the extent that a reaction is away from equilibrium: first, in an analytic approach we extend on the original work by Kacser and Burns (1973), and Noor et al. (2014), Dai and Locasale (2018); second, we relax the constraints necessary for the analytical solution and test the generality of the analytic solutions in demonstration models; and third, we analyse the kinetic models in the Biomodels and JWS Online databases.

2. Materials and methods

All calculations were performed using Mathematica, (Wolfram Research, Inc., Mathematica, Version 13.2, Champaign, IL (2022)).

Models were retrieved from Biomodels and JWS Online in SBML (Hucka et al., 2003) format, using their APIs, and converted to Mathematica readable format using the built-in conversion functionality of JWS Online.

Steady states, elasticities and control coefficients were calculated using the Mathematica packages employed by JWS Online. These functions involve linear algebra methods as described in Hofmeyr (2001).

Products, substrates and the mass action ratio of reactions were identified using the N-matrix structure of a reaction network (e.g. Hofmeyr, 2001). For reversible rate equations, symbolic K_{Eq} solutions were obtained by setting the equation equal to zero and solving symbolically for a product. Similarly, K_M symbols were identified through a combination of symbolic substitutions in rate equations, and string queries on parameter names in each model.

Standard Mathematica functions were used for numerical integration of the ODE models, and steady states were calculated using the FindRoot function. Flux control coefficients were calculated via the elasticity matrix inversion method (e.g. Hofmeyr, 2001).

3. Results

Enzyme kinetic rate equations can in general be split up into a maximal rate, a thermodynamic factor, and a kinetic factor (Hill, 1977; Westerhoff and van Dam, 1987; Rohwer and Hofmeyr, 2010; Noor et al., 2013). In an analytic approach we analysed the two extreme conditions where the enzymes are either completely saturated with substrate or product, or where both substrate and product have much lower concentrations than their K_M values.

3.1. MCA analytic approach

The simplest possible network would be the connection of two reactions via a common intermediate; reaction 1: S → X, reaction 2: X → P. A flux control coefficient quantifies the extent to which a reaction i controls the steady state flux (J) and is defined (Burns et al., 1985) as:

$$C_i^J = \frac{\partial J/J}{\partial E_i/E_i} \tag{1}$$

with E_i the amount of enzyme, or the maximal rate of the enzyme.

Using the summation and connectivity theorems of MCA (Kacser and Burns, 1973; Westerhoff and Chen, 1984), control coefficients can be expressed in terms of local properties, the elasticity coefficients:

$$\epsilon_y^i = \frac{\partial v_i/v_i}{\partial y/y} \tag{2}$$

where y is the concentration of any metabolite Y.

The two flux control coefficients of the simple two enzyme pathway can be expressed in terms of elasticities as follows:

$$C_1^J = \frac{\epsilon_x^2}{\epsilon_x^2 - \epsilon_x^1} \tag{3}$$

$$C_2^J = \frac{-\epsilon_x^1}{\epsilon_x^2 - \epsilon_x^1} \tag{4}$$

Using the definition above (Eq. (2)) one can express the elasticities in terms of enzyme kinetic parameters by taking the partial derivative of the reaction rate equation with respect to x, and normalizing for the steady state values of x and v. We can illustrate this for a uni-uni reaction ($S \rightarrow X$) using the generic equation (Hill, 1977; Westerhoff and van Dam, 1987; Rohwer and Hofmeyr, 2010) in which the rate equals the arithmetic product of the maximum rate (V_M), the extent of saturation with the substrate (the 'kinetic factor', ϕ_s), and 1 minus the disequilibrium ratio ($1-\rho$):

$$v = V_M \cdot \phi_s \cdot (1-\rho) \tag{5}$$

$$\text{with} \quad \rho = \frac{\Gamma}{K_{Eq}} = \frac{x/s}{K_{Eq}} = e^{\frac{\Delta G}{R \cdot T}} \tag{6}$$

$$\phi_s = \frac{s/K_S}{1 + s/K_S + x/K_X} \tag{7}$$

with, $s = [S], x = [X], K_{Eq} = x_{Eq}/s_{Eq}, \Delta G$ = Gibbs free energy change of reaction < 0, K_S and K_X represent the Michaelis constants (K_M's) for S and X, respectively. Since we here define pathway reaction such that reaction rates are positive, ρ lies between 0 (far from equilibrium) and 1 (near equilibrium).

This yields for the first reaction of our simple system:

$$v_1 = V_{1,M} \cdot \frac{s/K_{1,S}}{1 + s/K_{1,S} + x/K_{1,X}} \cdot (1-\rho) \tag{8}$$

with an elasticity for X (its product):

$$\epsilon_x^1 = \frac{-\rho_1}{1-\rho_1} - \frac{x/K_{1,X}}{1 + s/K_{1,S} + x/K_{1,X}} \tag{9}$$

and similarly for the second reaction, for which X is the substrate:

$$\epsilon_x^2 = \frac{1}{1-\rho_2} - \frac{x/K_{2,X}}{1 + x/K_{2,X} + p/K_{2,P}} \tag{10}$$

The first term on the right hand side of these expressions is the thermodynamic part, and the second term the kinetic part of the elasticity coefficient. The kinetic part can vary between 0 (i.e. $x \ll K_{1,X}$, $x \ll K_{2,X}$, when enzymes are completely unsaturated with pathway intermediates), and 1 (completely saturated), and the thermodynamic part can vary between 1 (in absence of product, $\rho = 0$) and infinity (at equilibrium, $\rho = 1$) for reaction substrate, and between 0 and minus infinity for the product.

Let us consider these extreme conditions, first the unsaturated case (i.e. the binding term equals 0), where the elasticities are completely described by the thermodynamic part of the equation:

$$\lim_{K_X \to \infty} \epsilon_x^1 = \frac{-\rho_1}{1-\rho_1} \qquad \lim_{K_X \to \infty} \epsilon_x^2 = \frac{1}{1-\rho_2} \tag{11}$$

By substituting the respective expressions for the elasticities in Eqs. (3) and (4) we obtain:

$$\lim_{K_X \to \infty} C_1^J = \frac{1-\rho_1}{1-\rho} \qquad \lim_{K_X \to \infty} C_2^J = \frac{\rho_1 \cdot (1-\rho_2)}{1-\rho} \tag{12}$$

with ρ defined as the product of the disequilibrium ratios of the respective steps in the pathway, i.e. $\rho_1 \cdot \rho_2$, being a measure for the

extent to which the pathway is away from equilibrium. The equation can be extended to a linear pathway with n reactions:

$$\lim_{K_X\to\infty} C_k^J = \begin{cases} \dfrac{1-\rho_1}{1-\rho} & \text{for } k=1 \\ \dfrac{1-\rho_k}{1-\rho}\cdot\prod_{i=1}^{k-1}\rho_i & \text{for } 1<k\le n \end{cases} \tag{13}$$

For the case of unsaturated enzymes in a linear pathway, a relation for ratios of control coefficients was derived in Kacser and Burns (1973) and in Noor et al. (2014), and a discussion of the consequences was given in Fell (1997), but no explicit expression for the individual control coefficients, as in Eq. (13), was given, nor was the extent to which the pathway as a whole is away from equilibrium taken into account. Note that ρ is a pathway property and can be calculated without detailed knowledge of all the steps.

Let us now consider the case where the enzymes are saturated by their substrates but not their products, i.e. where dissociation constants (K_M's) for the substrates are much lower than the substrate concentrations, making the kinetic term zero for Eq. (9), and 1 for Eq. (10):

$$\lim_{\substack{K_S\to 0\\ K_X\to\infty}} \epsilon_x^1 = \frac{-\rho_1}{1-\rho_1} \tag{14}$$

$$\lim_{\substack{K_X\to 0\\ K_P\to\infty}} \epsilon_x^2 = \frac{\rho_2}{1-\rho_2} \tag{15}$$

and:

$$\lim_{\substack{K_S\to 0\\ K_X\to\infty}} C_1^J = \frac{1-\rho_1}{\rho_1\cdot(1/\rho_1+1/\rho_2-2)} \tag{16}$$

$$\lim_{\substack{K_X\to 0\\ K_P\to\infty}} C_2^J = \frac{1-\rho_2}{\rho_2\cdot(1/\rho_1+1/\rho_2-2)} \tag{17}$$

For a linear pathway, consisting of n steps:

$$\lim_{\substack{K_{sub}\to 0\\ K_{prod}\to\infty}} C_k^J = \frac{1-\rho_k}{\rho_k\cdot(\sum_{i=1}^{n} 1/\rho_i - n)} \tag{18}$$

$$\lim_{\substack{K_{sub}\to 0\\ K_{prod}\to\infty}} C_k^J = \frac{1}{n}\cdot\frac{1-\rho_k}{\rho_k}\cdot\frac{1}{\langle 1/\rho_i\rangle - 1} \tag{19}$$

with $\langle 1/\rho_i\rangle$, the mean of $1/\rho_i$ of the reactions in the system. In Eq. (19) the order of the reactions is not important, but the extent that ρ_k for reaction k differs from the average ρ_i, is. If all ρ_i are equal (i.e. $\rho_k\cdot\langle 1/\rho_i\rangle = 1$) the equation reduces to $1/n$, i.e. flux control is equally distributed over the enzymes. For low values of ρ_k, and high values of ρ_i, the control approaches 1 for reaction k and 0 for the other reactions. Eq. (19) never exceeds $(1-\rho_k)/(1-\rho)$.

We also tested the case with high dissociation constants for substrates and low dissociation constants for products (i.e. binding term 1 for Eq. (9), and 0 for Eq. (10)), yielding the relationship:

$$\lim_{\substack{K_{sub}\to\infty\\ K_{prod}\to 0}} C_k^J = \frac{1}{n}\cdot\frac{1-\rho_k}{1-\langle\rho_i\rangle} \le \frac{1-\rho_k}{1-\rho} \tag{20}$$

The latter inequality provides the same bound as for the previous case, which can easily be shown for $n=2$ but also holds for longer pathways. For this case of product saturation, the flux control coefficients are again not determined by the position in the pathway, but rather by the pathway length, and by the extent that the reaction is further away from equilibrium than the average extent that reactions in the pathway are away from equilibrium: flux control should be distributed with more control in enzymes that catalyze the farther from equilibrium reactions.

That the extreme constraints of either very high, or very low binding constants for substrates/products, lead to the same boundary of the solution space for C_i^J and ρ_i is promising for the possibility of a generic solution, but we need to test the effect of relaxing the constraints to more realistic scenario's, for which no analytical solution can be given.

3.2. Numerical analysis of a randomized linear pathway with reversible reactions

A linear pathway consisting of four reversible reactions (rate equations as in Eq. (8)) was analysed numerically in terms of flux control (C_i^J) and disequilibrium ratio ($\rho_i = \Gamma_i/K_{eq_i}$). We tested in a large number of models, how either high/low or realistic values for K_S and/or K_P affect the relationship between C_i^J and ρ_i. In the following section, when we refer to high or low K_S, K_P, K_M, we used either 100000 or 0.00001 as values in the simulations. When we mention a narrow or wide distribution, we refer to a parameter sampling from a natural log (ln) normal distribution (derived from a normal distribution with a given mean and standard deviation), for the narrow distribution we used a mean of 1 and standard deviation of 0.2, leading to values between 1 and 5; and for the wide distribution we used a mean of 1 and standard deviation of 2, leading to values between 0.001 and 5000. For all simulations the external metabolite concentrations, i.e. of pathway substrate and product, were set at 10 and 1 respectively, and the K_M's at the specified values.

3.2.1. High K_M values

We started with high K_M values for both substrates and products, with a narrow parameter sampling distribution for the other parameters (i.e. V_M and K_{Eq} values). The result for 2000 simulations showed a distinct clustering for the four enzymes, shown in Fig. 1a, following the order in the pathway (black, red, blue, green) with the highest control for the first and lowest control for the last enzyme. A very strong correlation between C_i^J and ρ_i was observed for the first enzyme following the functional relation $f(x) : 1-\rho_i$, in agreement with Eq. (13) for small ρ (only solutions with $\rho < 0.01$ are shown).

When V_M and K_{Eq} values are sampled from a wider distribution, the clustering for the four enzymes is less clear, but the same functional relationship for the first enzyme is observed, and enzymes further down the pathway have less control (Fig. 1b). Again for all simulations with $\rho < 0.01$, all $C_i^J \le (1-\rho_i)$. The strong correlation observed for the first enzyme was shown to be completely dependent on the high K_P value: if this value is lowered (results for a value of 1 are shown in Fig. 1c), the strong effect of the position in the pathway is lost, although the last enzyme tends to have less flux control.

In a last set of simulations with high K_M values, we tested the effect of ρ by selecting solutions with $0.5 \le \rho \le 0.75$, which clearly showed the effect of ρ in the denominator of Eq. (13) for larger ρ values (Fig. 1d). Note that only for very short pathways ρ will have a value significantly close to 1. Even a single reaction that is far from equilibrium will make ρ insignificant in the (1-ρ) term. Typical ρ values when sampling parameters from the wide distribution fall between 10^{-6} and 1. Note that with higher K_{Eq} values (e.g. sampled from LogNormalDistribution[3, 2], with mean 3 and standard deviation 2), leading to ρ values between 10^{-9} and 10^{-3}, which are more realistic for metabolic pathways such as glycolysis, the clustering as seen in Fig. 1a falls away and a result very similar to Fig. 1b is observed.

3.2.2. Interchanging high - low K_S - K_P values

Next we studied models for the four enzyme pathway with first low K_S and high K_P values, and second high K_S and low K_P values, using similar scenarios as in Section 3.2.1. When V_M and K_{Eq} are sampled from a narrow distribution, for both cases a distinct clustering for the reactions is observed in the C_i^J versus ρ_i plot (Fig. 2a, b), without the strong effect of the position of the reaction in the pathway. When the parameters are sampled from a wider distribution, the clustering is less tight (Fig. 2c, d) and a result similar to Fig. 1c is observed.

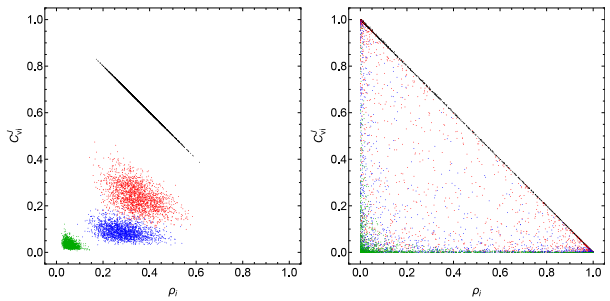

(a) High K_S, high K_P values other parameters narrow distribution

(b) High K_S, high K_P values other parameters wider distribution

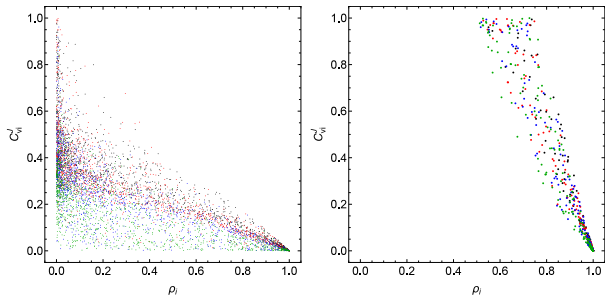

(c) High K_S, $K_P = 1$ values other parameters wider distribution

(d) High K_S, high K_P values solutions with $0.5 < p < 0.75$

Fig. 1. C_i^J *versus* ρ_i *at high* K_M *values.* For a four step linear pathway model 2000 steady states were analysed for each of the panels, where V_M and K_{Eq} values were sampled from a LogNormalDistribution[1,0.2] (a) and LogNormalDistribution[1,2] (b), except for K_S and K_P which were set at 100000. In (c) $K_P = 1$, and all other parameters chosen as in (b). In (d) K_{Eq} values were sampled from a LogNormalDistribution[1,3], and all other parameters chosen as in (b). Only solutions with the pathway disequilibrium ratio $\rho < 0.01$ are shown in (a,b,c), the effect of selecting $0.5 < \rho < 0.75$ is shown in (d). Solutions for the enzymes 1 to 4 in the pathway are shown in black, red, blue and green, respectively.

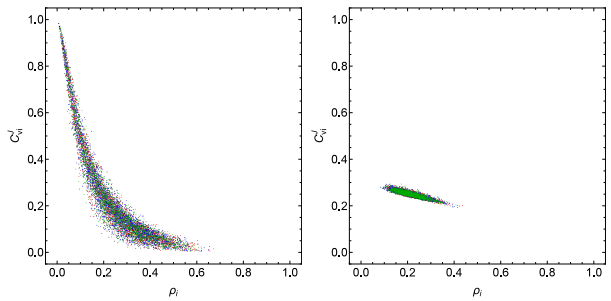

(a) Low K_S, high K_P values other parameters narrow distribution

(b) High K_S, low K_P values other parameters narrow distribution

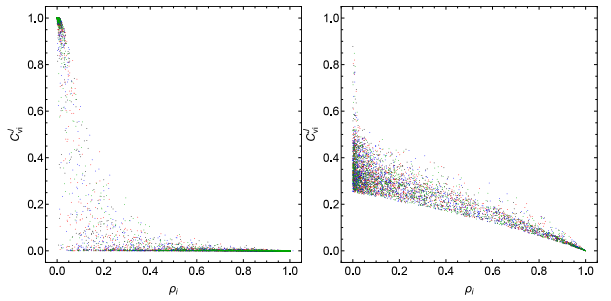

(c) Low K_S, high K_P values other parameters wider distribution

(d) Low K_S, high K_P values other parameters wider distribution

Fig. 2. C_i^J *versus* ρ_i *with low* K_M *values.* For a four step linear pathway model 2000 steady states were analysed for each of the panels, with K_S and K_P set at either high or low values (i.e. 100000 or 0.00001) respectively, as indicated under the panels, and V_M and K_{Eq} were sampled from a narrow distribution (a, b), or a wide distribution (c, d). Only solutions with the pathway disequilibrium ratio $\rho < 0.01$ are shown. Solutions for the enzymes 1 to 4 in the pathway are shown in black, red, blue and green, respectively.

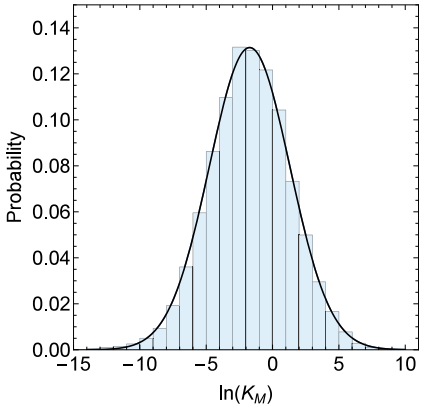

Fig. 3. K_M *values from the Brenda database.* All entries from the Brenda database (date: 9 May 2023, 162856 hits with a median value of 0.18), were imported in Mathematica and a normal distribution was fitted to the natural logarithm of the K_M values, with a mean and standard deviation of −1.73 and 3.04 respectively. The probability density function (PDF) of the normal distribution is plotted together with a histogram of the log values.

3.2.3. Brenda K_M values

The analytical solutions given in Eqs. (13) and (19) where restricted to either high or low K_M values, and although the numerical solutions showed quite similar results for both constraints, particularly for low ρ values and when a wider distribution was sampled for the other parameters, it is important to investigate the solution space for more realistic K_M values. For this we queried the Brenda database (Chang et al., 2020) for K_M values and saved the 162 000 hits. The $\ln(K_M)$ values could be well described with a normal distribution (Fig. 3), and the fit was used to sample for more realistic K_M values.

With the more realistic K_M values, and the other parameters sampled from a narrow distribution, we obtained a result (Fig. 4a) similar to that obtained in Fig. 2a, with a concentration of C_i^J values at the $1/n = 0.25$ area. As before, the solution distribution could be stretched and moved closer to the y-axis by sampling kinetic parameters (other than the K_M values, for which the Brenda distribution was used) from a wider distribution, Fig. 4b.

The numerical analysis of the simple linear pathway showed that in most scenarios no strict functional relationship exists between C_i^J and ρ_i, but some interesting correlations could be observed. For pathways that have a small overall disequilibrium ratio e.g. $\rho < 0.01$, $C_i^J < (1-\rho_i)$. And secondly, smaller overall ρ values pushed the distribution closer to the axes, i.e. it is very unlikely to have a $C_i^J > 0.5$ with a $\rho_i > 0.2$.

3.2.4. Branched core model

We tested the same conditions of the kinetic and thermodynamic terms on a 5 reactions branched model, consisting of an input reaction to a branch point metabolite, and then two reactions in each of the branches. Branched pathways are different from linear pathways in a number of ways important for our analysis: first, there are multiple fluxes, so a flux control coefficient needs to be explicit on the flux; second, the concept of a pathway is not uniquely defined (with multiple fluxes there can be multiple pathways, one could for instance use elementary flux modes (Schuster and Hilgetag, 1994) as a method to define them); and last, for the expression of control coefficients in terms of elasticity coefficients, flux ratios over the branches come into play. Since in our analysis we focus on the flux control of an enzyme on its own flux, the first point is not an issue. For the calculation of

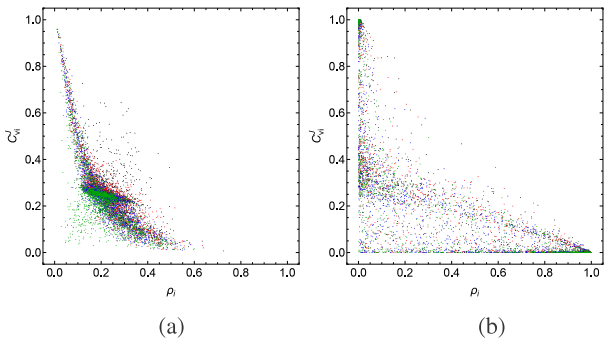

Fig. 4. C_i^J *versus* ρ_i *with realistic* K_M *values.* For a four step linear pathway model 2000 steady states were analysed for each of the panels, where the parameters were sampled from a narrow (a) or wide distribution (b), except for K_S and K_P which were sampled from the PDF shown in Fig. 3. Only solutions with the pathway disequilibrium ratio $\rho < 0.01$ are shown. Solutions for the enzymes 1 to 4 in the pathway are shown in black, red, blue and green, respectively.

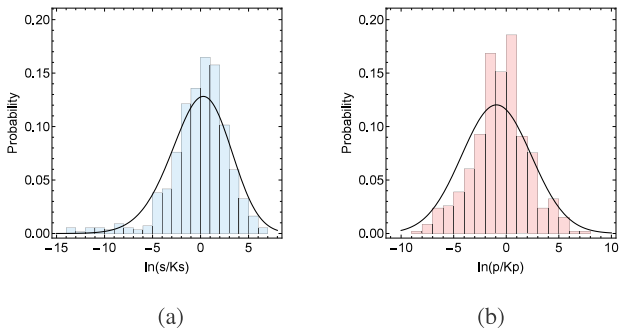

Fig. 5. *Substrate and product saturation for reactions in JWS Online and Biomodels databases.* For the selected reactions in which substrate or product and their binding constants could be identified, we analysed s/K_S and p/K_P at steady state (4286 and 509 reactions, respectively). For substrate binding a skewed normal distribution was fitted to the $\ln(s/K_S)$ values, with shape, location, and scale parameters of 2.5, 4.1, −1.3, (with a maximum probability for s/K_S of 1.3). For product binding a normal distribution was fitted to the $\ln(p/K_P)$ values, with a mean and standard deviation of −0.93, and 3.32, (with a maximum probability for p/K_P of 0.4).

the pathway disequilibrium ratio ρ we defined a pathway as running from external variables to the branch point metabolite. The third point is taken into account in our numerical analysis, but precludes (in combination with the number of reactions) an analytical analysis as we did for the linear pathway.

The simulation results for the branched pathway, resulted in essentially the same results as we obtained for the linear pathway. The $(1-\rho_i)/(1-\rho)$ line formed the upper boundary for the solutions and we observed the same type of clustering. When the flux through one of the branches was significantly lower than the flux through the other branch, the flux control of the first enzyme in the branch approached the $(1-\rho_i)/(1-\rho)$ line for the high K_S and high K_M case.

3.3. Analysis of models in the JWS Online and Biomodels databases

We set up a workflow to find a complement of all Biomodels and JWS Online models, and compared the results for the numerical simulations in the core model with the results obtained with the published models, and so tested the validity of the constraints imposed in the analytic solution.

3.3.1. Selection of models and reactions

A number of criteria were applied to select models from the total list: (1) we only used published models, so only included the curated models from the Biomodels database and excluded the demonstration models in JWS Online; (2) we only analysed kinetic models, i.e. no stoichiometric models; (3) we did not include models defined in terms of rate rules or algebraic rules; (4) we excluded models that are part of a development series, and only used the final model of such a series, e.g. of the eighteen models published in Smallbone et al. (2013) we only used model 18; (5) we excluded a few models that describe a single enzyme reaction.

After the initial selection we tested 1149 models with 27 101 reactions. For the models we made additional selections by excluding models with events, piecewise functions, or that were oscillatory, which left us with 691 models. Of these models, 561 reached a steady state, and only these were then used because we here limit ourselves to MCA of steady state fluxes. The vast majority of the initially selected (27 101) set of reactions, 23921 did not include a product inhibition term in the denominator, most (21 021) were described by mass-action kinetics, and less than half were modelled with reversible kinetics (8608).

3.3.2. Elasticities and substrate/product saturation

The analytical solutions indicated that the degree of saturation of enzymes has an effect on their flux control. Accordingly, we first analysed the degree of saturation at steady state in the reactions where a substrate or product Michaelis constant could be identified, as s/K_S and p/K_P, with median values of 1.2 and 0.6 respectively, with 90% of the values between 0.01 and 100 for both substrate and product. The distributions of $\ln(s/K_S)$ and $\ln(p/K_P)$ at steady state are quite similar, with maximum probability for values close to 1, and could be described with a normal distribution, with a slightly better fit with a skewed normal distribution for $\ln(s/K_S)$ (Fig. 5).

Elasticities with respect to substrates and products for irreversible enzymes are dependent on the degree of saturation and this is illustrated in Fig. 6a with values decreasing from 1 to 0 as substrate concentration increases from 0 to saturation, while the product elasticity decreases from 0 to −1 as the product concentration increases from 0 to saturation (Fig. 6b). The equation $f(s/K_S) = (1+p/K_P)/(1+s/K_S+p/K_P)$, (the substrate elasticity of an irreversible Michaelis Menten equation with product inhibition) fits most of the substrate elasticities data well for $p = 0$, because many of the irreversible reactions in the model databases do not include a product in the denominator (78 of the 145 reactions), but the presence of product has an effect on the relationship, indeed as indicated in Fig. 6a where the reactions that include product in the denominator of the rate equation, are indicated by the red data points. For the product elasticity, the relationship $f(p/K_P) = (-p/K_P)/(1+s/K_S+p/K_P)$, (the product elasticity of an irreversible Michaelis Menten equation with product inhibition) does not describe the data so well for $s = 0$, but whereas many irreversible reactions do not include product, all reactions include substrate and hence will tend to show a less negative elasticity with respect to the product, as observed in Fig. 6b, (79 reactions).

For the reversible reactions the elasticities have a much larger range and are strongly dependent on the ρ_i value of the reaction (Fig. 6c (1794 reactions) and d (621 reactions)), see also Rohwer and Hofmeyr (2010) and Noor et al. (2013) for a more complete treatment. Whereas the binding term is important at low ρ_i values, as it can bring the elasticity down with a value of 1, this effect becomes insignificant at higher ρ_i values, where the elasticities become functions of the Gibbs free energy change of reaction only.

3.3.3. Control versus thermodynamics

For the reversible reactions for which the disequilibrium ratio could be analysed (443 reactions), we plotted $C_i^{J_i}$ versus ρ_i (see Fig. 7), ρ_i is 1 at equilibrium and smaller than 1 for forward flux through the

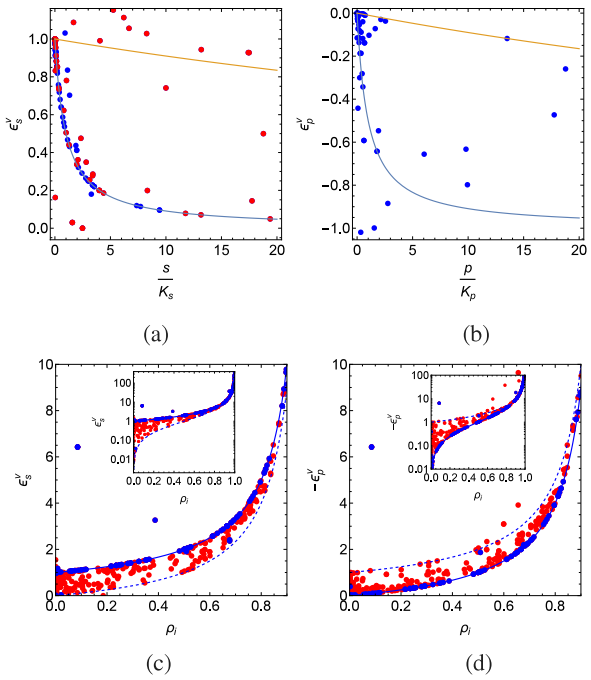

Fig. 6. *Elasticities for substrate and product as a function of saturation or disequilibrium ratio.* Elasticities with respect to substrate and product were calculated, and analysed as a function of the extent of saturation of the enzyme (s/K_S and p/K_P) for the irreversible reactions (a, b), or as a function of the ρ_i for reversible enzymes (c, d). Note that in (d) the negative value of the product elasticity is plotted, to allow for the log axis in the inset. In (a) the function $f(x) : (1 + p/K_P)/(1 + s/K_S + p/K_P)$ is plotted with $p/K_P = 0$ or 100 (blue and yellow line respectively). The red symbols in (a) denote reactions that include a product term in the denominator. In (b) the function $f(x) = -(p/K_P)/(1 + s/K_S + p/K_P)$ is plotted with $s/K_S = 0$ or 100 (blue and yellow line respectively). In (c) the functions $f(x) = 1/(1 - \rho_i)$ and $f(x) = \rho_i/(1 - \rho_i)$, (which can be derived from Eq. (10) by setting the kinetic term to either 0 or 1) are plotted with solid and dashed blue lines respectively. In (d) the functions $f(x) = \rho_i/(1 - \rho_i)$ and $f(x) = 1/(1 - \rho_i)$, (which can be derived from Eq. (9) by multiplying by −1 and setting the kinetic term to either 0 or 1) are plotted with solid and dashed blue lines respectively.

pathway. As was seen for the simple core models in 3.2, many reactions cluster at either high (i.e. close to 1; near equilibrium reactions) or low (i.e., close to zero; far from equilibrium reactions) values for ρ_i and have a low flux control coefficient. The vast majority of reactions with $C_i^{J_i} > 0.3$ have a $\rho_i < 0.2$, and in almost all cases $C_i^{J_i} < (1 - \rho_i)$. There was no clear effect of having a product term in the denominator of the rate equation, compared to reactions with only a product term in the numerator (indicated in Fig. 7 by blue and red symbols respectively), or for reactions that are allosterically regulated (green symbols), on the relationship between $C_i^{J_i}$ versus ρ_i. However, there is a tendency for reactions without a product term in the denominator to be clustered stronger near equilibrium, while the reactions without a product term, and the allosterically regulated enzymes are more concentrated far away from equilibrium.

The few exceptions that lie significantly above the $(1 - \rho_i)$ line are parallel reactions that carry a low flux. This will tend to give these reactions a high flux control over their own reaction, even with high ρ_i values, as their substrate and product are buffered by the main flux in the pathway.

It is clear from Fig. 7 that the vast majority of reactions have a flux control smaller than 1. From an MCA perspective this is not so surprising, as the flux control coefficients of all reactions on any flux sum up to one, and the control is likely to be distributed. Nonetheless, it is interesting to investigate what caused the change in flux over the reaction step to be less than proportional to the change in the enzyme activity.

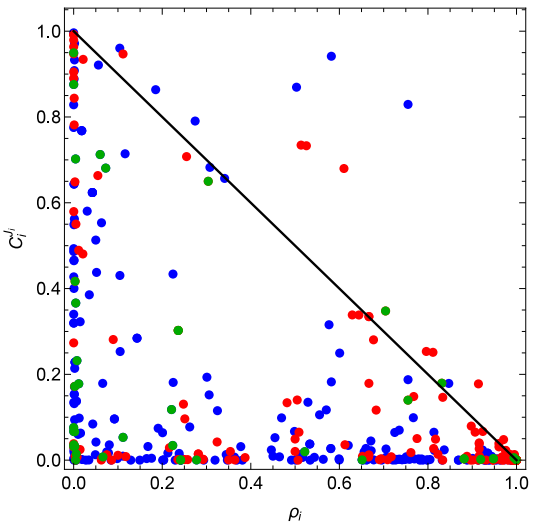

Fig. 7. *Correlation between $C_i^{J_i}$ and ρ_i for models from JWS and Biomodels.* For the selected 443 reactions (see main text for details), $C_i^{J_i}$ is plotted as a function of ρ_i. Blue symbols denote reactions that have a product term in the denominator, while the red symbols (180 in total) have the product term only in the numerator (e.g. reversible mass action kinetics). The green symbols denote reactions with allosteric regulation (40 in total). The black line is the y(x = 1-x function.

We see a relation between the extent a reaction is away from equilibrium and its flux control, but the mechanism via which this reflects in the flux control coefficient is not yet clear. The lower than proportional change in flux must be due to a change in the concentration of an effector of the enzyme, e.g. substrate, product or allosteric regulator:

$$C_i^{J_i} = 1 + C_i^s \epsilon_s^i + C_i^p \epsilon_s^i + C_i^r \epsilon_r^i. \tag{21}$$

We analysed the contributions of changes in substrate, product and allosteric regulators on the flux control (see Eq. (21)) for the enzymes in the JWS Online and Biomodels databases. The analysis showed (Fig. 8) that the contribution of the product term $C_i^p \epsilon_s^i$ is smaller than that of the substrate term $C_i^s \epsilon_s^i$. The $C_i^r \epsilon_r^i$ term is a bit more complicated because the allosteric regulation (i.e. ϵ_r^i) can be positive or negative, and the effect of perturbing v_i can lead to an increase or decrease in the concentration of the regulator (C_i^r). Further splitting up the response terms in Eq. (21) in elasticity and concentration control coefficients, showed that the absolute values of elasticities for substrate and product have a wide distribution (due to the reactions close to equilibrium, see also Fig. 6) with a slightly higher value for the substrates. The elasticities for the allosteric regulator have a much narrower range, from −3 to 3. The concentration control coefficients for substrates were larger than for products, with an intermediate value for allosteric regulators (mean absolute values of 0.29, 0.13 and 0.21 respectively). Thus, in the reactions analysed here, the change in substrate concentration upon an enzyme perturbation was the strongest contributor to lowering the flux control coefficient.

4. Discussion

Our work extends on the original relationship as presented by Kacser and Burns (1973) for the "unsaturated" case, in a linear pathway:

$$C_1^J : C_2^J : C_3^J ... \equiv 1 - \rho_1 : \rho_1(1 - \rho_2) : \rho_1\rho_2(1 - \rho_3)...$$

In Noor et al. (2014) and Dai and Locasale (2018) similar approaches were followed to express flux control coefficients in terms of Gibbs free energy changes under conditions of enzyme saturation or sub-saturation, leading to expressions of ratios of control coefficients,

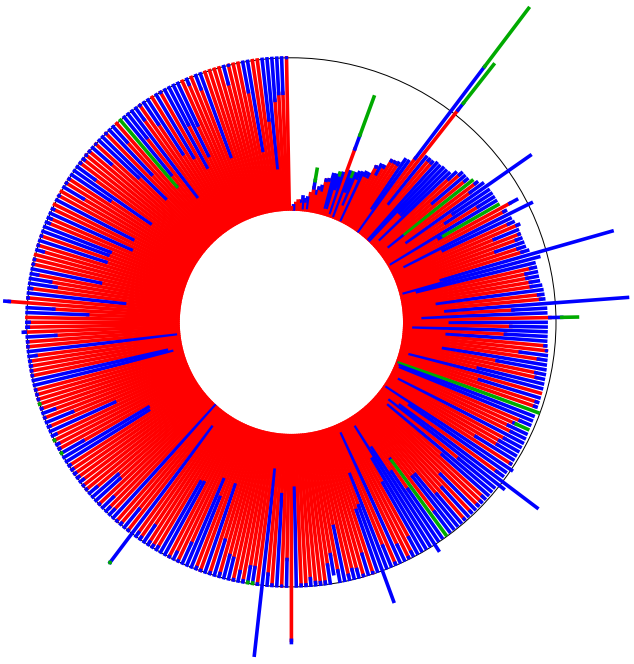

Fig. 8. *Contribution of substrate, product, and allosteric regulator changes to flux control.* For 341 reactions we analysed the contribution of substrate (red), product (blue), and allosteric regulator (green) responses ($C_i^x \cdot \epsilon_x^i$) to its flux control. The reactions are sorted according to their flux control, starting at the top, counter-clock wise, and 1- the sum of the responses for a reaction is equal to its flux control (Eq. (21)). Note that the responses are shown as absolute values and in a few cases the absolute value does not reflect the proper sign. Substrate and product responses are negative (in the vast majority of cases), while the regulatory can be positive or negative. The radius difference between the outer and inner circle equals 1, and thus, the difference between the summed responses and the outer circle reflects the flux control for the specific reaction (with the above mentioned few exceptions). The majority of the reactions have a small flux control (i.e. $C_1^J < 0.1$ for 80% of the reactions), and for most reactions the substrate response loop has the strongest effect. Only 22 reactions have an allosteric regulatory response loop.

or a scaling factor (proportionality constant), e.g. in Noor et al. (2014), $C_i^J = \alpha(e^{-g_i} - 1)(\prod_{m=1}^{i} e^{-g_m})^{-1}$, where α is determined by the summation theorem but is not made explicit in terms of the pathway disequilibrium ratio (ρ), as we did in Eq. (13).

In Dai and Locasale (2018) a thermodynamic driving force (TDF) is defined as "the deviation from the thermodynamic equilibrium by the reaction free energy change that is closest to zero", and subsequently cases are analysed where TDF $\rightarrow -\infty$. For these cases they find that the first enzyme always has full flux control. The condition TDF $\rightarrow -\infty$ is unnecessary stringent, as it constraints all ρ_i to be very small, and indeed, then the first enzyme has full flux control (i.e. Eq. (13), for ρ_1 and ρ close to 0). From our analysis it is clear that even if one reaction step is far from equilibrium (i.e. this makes ρ close to 0) the flux control coefficient for step i (in the case of the linear pathway, in the unsaturated state) is given by $1-\rho_i$. In that case it is not necessarily the first enzyme that has full flux control, the flux control is distributed over the enzymes before (and including) the reaction that is far away from equilibrium (Eq. (13)).

Making the expression explicit in ρ is important as it is possible to calculate ρ from the chemical potential of pathway products and substrates only, i.e. no information on the pathway intermediates is necessary.

The analytic treatment was restricted to linear pathways, and it is important to consider branches. In Dai and Locasale (2018) branched pathways were simulated in computer models, and we also simulated a simple branched system to test our analysis results for such systems. Branched systems are harder to analyse in the thermodynamic approach as flux ratios come into play when expressing control coefficients in terms of elasticity coefficients (Fell and Sauro, 1985). We resolved this issue largely by focussing on the flux control of a step on its own flux. However, the concept of a pathway disequilibrium ratio is not well defined for a branched pathway, as one can define more than one pathway, not necessarily with the same ρ. For our analysis one needs to take the ρ for each branch into account, i.e. a branch is a separate pathway, starting from the branch point intermediate and extend to the product of the branch. When doing so our analysis holds for branched pathways.

A branch can become isolated from the rest of the system when there is a large difference in flux between the "main" pathway and the branch. The reason for this is that the enzymes in the branch will tend to have very low concentration control on the branch-point intermediate, and therefore the branch operates as if in isolation from the main pathway, (and the flux control coefficients of the enzymes in the branch on the branched pathway flux will add up to 1). Clearly, a branched pathway can have more than one interaction with the main pathway, for instance co-factors such as NAD(P)H and ATP tend to link reactions between different pathways, but generally speaking, if the branch pathway contributes only to a small extent in the total turn-over of the co-factors, which will most likely be the case due to its low flux value, the branches will tend to operate in isolation from the rest of the system.

Probably the most important component of our study is the analysis of over 1000 models that were retrieved from the JWS Online and Biomodels databases. Although most models did not lend themselves to steady state analysis, and for many reactions irreversible kinetics were used, we could still analyse a large number (443) of reactions in terms of disequilibrium ratio and flux control. The results showed that for the vast majority of reactions (i.e. 94%) the relationship between $C_i^{J_i}$ and ρ_i was in good agreement with the boundary conditions given in the analytical derivation, i.e. $C_i^{J_i} < (1-\rho_i)/(1-\rho)$. Thus, the disequilibrium ratio gives a good indication on the maximal flux control an enzyme can have, 75% of the reactions with a $C_i^{J_i} > 0.2$ had a $\rho_i < 0.2$, and 83% of the reactions with a $C_i^{J_i} > 0.4$ had a $\rho_i < 0.2$. So, the controversial Rolleston criterion of $\rho_i < 0.2$, is a fair indicator to identify steps that potentially have flux control, but in general the ρ_i can merely point at a maximal flux control, and not serve so much as an estimator for a flux control coefficient.

In our analysis we added more nuance to the $\rho_i < 0.2$ criterion, by pointing out that it must be compared to the pathway disequilibrium ratio ρ. If a pathway as a whole has a fairly high ρ, which is unlikely for long pathways, but could happen in short branches, then an enzyme with a $\rho_i > 0.2$ can have a high flux control, but it is unlikely to be higher than $(1-\rho_i)/(1-\rho)$. We only saw a few cases where $C_i^{J_i}$ was significantly larger than $(1-\rho_i)/(1-\rho)$. In these instances substrates and products of the reaction were strongly buffered, in effect isolating the reaction from the rest of the system, and this will lead to a high flux control for the reaction. The examples we saw were models where fluxes through iso-enzymes were distinguished, and when one of the iso-enzyme has a much lower flux than the other then its substrate and product will be buffered.

So, to come back to our original question in the title: "Is the extent a reaction is away from equilibrium a good indicator for its flux control?", we can answer that the ρ_i of a reaction is not a good estimator for its flux control coefficient, but it indicates an upper value for $C_i^{J_i}$, which generally does not exceed $(1-\rho_i)/(1-\rho)$. The pathway disequilibrium will generally have a low value, reducing the upper boundary to $1-\rho_i$. We analysed the $C_i^{J_i}$ for a large number of reactions from curated models from the JWS Online and Biomodels databases, and the vast majority of reactions were well below the $1-\rho_i$ line.

Funding

This work was part funded by the DST/NRF in South Africa, particularly the SARChI initiative (NRF-SARCHI-82813) and the SRUG2204173612 grants.

Declaration of competing interest

The authors declare that they have no known competing financial interests or personal relationships that could have appeared to influence the work reported in this paper.

Acknowledgments

We wish to thank David Fell for valuable discussions during the study, and in particular for pointing to relevant research papers, and for suggesting to separate out product effects in the thermodynamic and kinetic terms.

References

Alberghina, Westerhoff (Eds.), 2005. Systems Biology. In: Topics in Current Genetics, (no. 13), Springer Berlin, Heidelberg, http://dx.doi.org/10.1007/b95175.

Alm, R., Waltemath, D., Wolfien, M., Wolkenhauer, O., Henkel, R., 2015. Annotation-based feature extraction from sets of SBML models. J. Biomed. Semant. 6 (1), 20. http://dx.doi.org/10.1186/s13326-015-0014-4.

Bergmann, F.T., Sauro, H.M., 2008. Comparing simulation results of SBML capable simulators. Bioinformatics 24 (17), 1963–1965. http://dx.doi.org/10.1093/bioinformatics/btn319.

Burns, J.A., Cornish-Bowden, A., Groen, A.K., Heinrich, R., Kacser, H., Porteous, J.W., Rapoport, S.M., Rapoport, T., Stucki, J.W., Tager, J.M., Wanders, R.J.A., Westerhoff, H.V., 1985. Control analysis of metabolic systems. Trends Biochem. Sci. 10, 16.

Chang, A., Jeske, L., Ulbrich, S., Hofmann, J., Koblitz, J., Schomburg, I., Neumann-Schaal, M., Jahn, D., Schomburg, D., 2020. BRENDA, the ELIXIR core data resource in 2021: new developments and updates. Nucleic Acids Res. 49 (D1), D498–D508. http://dx.doi.org/10.1093/nar/gkaa1025.

Dai, Z., Locasale, J.W., 2018. Thermodynamic constraints on the regulation of metabolic fluxes. J. Biol. Chem. 293 (51), 19725–19739. http://dx.doi.org/10.1074/jbc.ra118.004372.

Fell, D., 1997. Understanding the control of metabolism.

Fell, D.A., Sauro, H.M., 1985. Metabolic control and its analysis. Eur. J. Biochem. 148 (3), 555–561. http://dx.doi.org/10.1111/j.1432-1033.1985.tb08876.x.

Groen, A.K., Wanders, R.J.A., Westerhoff, H.V., van-der-Meer, R., Tager, J.M., 1982. Quantification of the contribution of various steps to the control of mitochondrial respiration. J. Biol. Chem. 257, 2754–2757..

Heinrich, R., Rapoport, T.A., 1974. A linear steady-state treatment of enzymatic chains. Eur. J. Biochem. 42 (1), 89–95. http://dx.doi.org/10.1111/j.1432-1033.1974.tb03318.x.

Hill, T., 1977. Free Energy Transduction in Biology. Academic Press.

Hofmeyr, J.H., 2001. Metabolic control analysis in a nutshell. In: Proceedings of the 2nd International Conference on Systems Biology. Omnipress, Wisconsin, pp. 291–300.

Hucka, M., Finney, A., Sauro, H.M., Bolouri, H., Doyle, J.C., Kitano, H., Arkin, A.P., Bornstein, B.J., Bray, D., Cornish-Bowden, A., Cuellar, A.A., Dronov, S., Gilles, E.D., Ginkel, M., Gor, V., Goryanin, I.I., Hedley, W.J., Hodgman, T.C., Hofmeyr, J.H., Hunter, P.J., Juty, N.S., Kasberger, J.L., Kremling, A., Kummer, U., Novère, N.L., Loew, L.M., Lucio, D., Mendes, P., Minch, E., Mjolsness, E.D., Nakayama, Y., Nelson, M.R., Nielsen, P.F., Sakurada, T., Schaff, J.C., Shapiro, B.E., Shimizu, T.S., Spence, H.D., Stelling, J., Takahashi, K., Tomita, M., Wagner, J., Wang, J., Forum, S., 2003. The systems biology markup language (SBML): a medium for representation and exchange of biochemical network models. Bioinformatics 19 (4), 524–531. http://dx.doi.org/10.1093/bioinformatics/btg015.

Jensen, P., Michelsen, O., Westerhoff, H., 1993. Control analysis of the dependence of E. coli physiology on the H+-ATPase. Proc. Natl. Acad. Sci. USA 90, 8068–8072.

Kacser, H., Burns, J.A., 1973. The control of flux. Symp. Soc. Exp. Biol. 27, 65–104.

Lambusch, F., Waltemath, D., Wolkenhauer, O., Sandkuhl, K., Rosenke, C., Henkel, R., 2018. Identifying frequent patterns in biochemical reaction networks: a workflow. Database 2018, bay051. http://dx.doi.org/10.1093/database/bay051.

Lloyd, C.M., Lawson, J.R., Hunter, P.J., Nielsen, P.F., 2008. The CellML model repository. Bioinformatics 24 (18), 2122–2123. http://dx.doi.org/10.1093/bioinformatics/btn390.

Newsholme, E.A., Gevers, W., 1967. Control of glycolysis and gluconeogenesis in liver and kidney cortex. Vitam. Horm. 25, 1–87.

Noor, E., Bar-Even, A., Flamholz, A., Reznik, E., Liebermeister, W., Milo, R., 2014. Pathway thermodynamics highlights kinetic obstacles in central metabolism. PLoS Comput. Biol. 10 (2), e1003483. http://dx.doi.org/10.1371/journal.pcbi.1003483.

Noor, E., Flamholz, A., Liebermeister, W., Bar-Even, A., Milo, R., 2013. A note on the kinetics of enzyme action: A decomposition that highlights thermodynamic effects. FEBS Lett. 587 (17), 2772–2777. http://dx.doi.org/10.1016/j.febslet.2013.07.028.

le Novere, N., Bornstein, B., Broicher, A., Courtot, M., Donizelli, M., Dharuri, H., Li, L., Sauro, H., Schilstra, M., Shapiro, B., Snoep, J.L., Hucka, M., 2006. BioModels database: a free, centralized database of curated, published, quantitative kinetic models of biochemical and cellular systems. Nucleic Acids Res. 34 (Database issue), D689–D691. http://dx.doi.org/10.1093/nar/gkj092.

Olivier, B.G., Snoep, J.L., 2004. Web-based kinetic modelling using JWS online. Bioinformatics 20 (13), 2143–2144. http://dx.doi.org/10.1093/bioinformatics/bth200.

du Preez, F., Conradie, R., Penkler, G., Holm, K., van Dooren, F., Snoep, J., 2008. A comparative analysis of kinetic models of erythrocyte glycolysis. J. Theoret. Biol. 252 (3), 488–496. http://dx.doi.org/10.1016/j.jtbi.2007.10.006.

Rohwer, J.M., Hofmeyr, J.H.S., 2010. Kinetic and thermodynamic aspects of enzyme control and regulation. J. Phys. Chem. B 114 (49), 16280–16289. http://dx.doi.org/10.1021/jp108412s.

Rolleston, F., 1972. A theoretical background to the use of measured concentrations of intermediates in study of the control of intermediary metabolism. Curr. Top. Cell. Regul. 5, 47–75. http://dx.doi.org/10.1016/b978-0-12-152805-8.50008-3.

Schuster, S., Hilgetag, C., 1994. On elementary flux modes in biochemical reaction systems at steady state. J. Biol. Systems 2 (02), 165–182. http://dx.doi.org/10.1142/s0218339094000131.

Smallbone, K., Messiha, H.L., Carroll, K.M., Winder, C.L., Malys, N., Dunn, W.B., Murabito, E., Swainston, N., Dada, J.O., Khan, F., Pir, P., Simeonidis, E., Spasić, I., Wishart, J., Weichart, D., Hayes, N.W., Jameson, D., Broomhead, D.S., Oliver, S.G., Gaskell, S.J., McCarthy, J.E., Paton, N.W., Westerhoff, H.V., Kell, D.B., Mendes, P., 2013. A model of yeast glycolysis based on a consistent kinetic characterisation of all its enzymes. FEBS Lett. 587 (17), 2832–2841. http://dx.doi.org/10.1016/j.febslet.2013.06.043.

Westerhoff, H.V., Chen, Y.D., 1984. How do enzyme activities control metabolite concentrations? Eur. J. Biochem. 142 (2), 425–430. http://dx.doi.org/10.1111/j.1432-1033.1984.tb08304.x.

Westerhoff, H.V., van Dam, K., 1987. Thermodynamics and control of biological free energy transduction.

Wittig, U., Rey, M., Weidemann, A., Kania, R., Mueller, W., 2018. SABIO-RK: an updated resource for manually curated biochemical reaction kinetics. Nucleic Acids Res. 46 (Database issue), D656–D660. http://dx.doi.org/10.1093/nar/gkx1065.

Wolstencroft, K., Krebs, O., Snoep, J.L., Stanford, N.J., Bacall, F., Golebiewski, M., Kuzyakiv, R., Nguyen, Q., Owen, S., Soiland-Reyes, S., Straszewski, J., van Niekerk, D.D., Williams, A.R., Malmström, L., Rinn, B., Müller, W., Goble, C., 2017. FAIRDOMHub: a repository and collaboration environment for sharing systems biology research. Nucleic Acids Res. 45 (D1), D404–D407. http://dx.doi.org/10.1093/nar/gkw1032.